Electronic Supplementary Material (ESI) for Soft Matter.

Supplementary Information

Transient Mechanical Interactions between Cells and Viscoelastic Extracellular Matrix

Brandon Slater[*]
Weldon School of Biomedical Engineering, Purdue University
206 S Martin Jischke Dr, West Lafayette, IN 47907

Jing Li[*]
Weldon School of Biomedical Engineering, Purdue University
206 S Martin Jischke Dr, West Lafayette, IN 47907

Dhiraj Indana[*]
Department of Mechanical Engineering, Stanford University
440 Escondido Mall, Stanford, CA, 94305, USA

Yihao Xie
School of Mechanical Engineering, Purdue University
585 Purdue Mall, West Lafayette, IN 47907

Ovijit Chaudhuri[§]
Department of Mechanical Engineering, Stanford University
452 Escondido Mall, Stanford, CA, 94305, USA

Taeyoon Kim[§]
Weldon School of Biomedical Engineering, Purdue University
206 S Martin Jischke Dr, West Lafayette, IN 47907
kimty@purdue.edu

* indicates equal contribution.
§ indicates corresponding authors.

SUPPLEMENTARY TEXT

Brownian dynamics based on the Langevin equation

The displacements of the cylindrical elements are governed by the Langevin equation with inertia neglected:

$$\mathbf{F}_i - \zeta_i \frac{\mathrm{d}\mathbf{r}_i}{\mathrm{d}t} + \mathbf{F}_i^{\mathrm{T}} = 0 \tag{S1}$$

where $\mathbf{r}_i$ represents the position of the ith element, ζ_i is a drag coefficient, $\mathbf{F}_i$ is a deterministic force, and t is time. The stochastic force $\mathbf{F}^{\mathrm{T}}{}_i$ satisfies the fluctuation-dissipation theorem [1]:

$$\left\langle \mathbf{F}_i^{\mathrm{T}}(t)\mathbf{F}_j^{\mathrm{T}}(t)\right\rangle = \frac{2k_{\mathbf{B}}T\zeta_i\delta_{ij}}{\Delta t}\boldsymbol{\delta} \tag{S2}$$

where δ_{ij} is the Kronecker delta, $\boldsymbol{\delta}$ is a second-order tensor, and Δt is a time step equal to 4×10^{-4} s in all simulations.

Drag coefficients are calculated using an approximated form for a cylindrical object [2]:

$$\zeta_i = 3\pi\mu r_{\mathrm{c},i}\frac{3+2r_{0,i}/r_{\mathrm{c},i}}{5} \tag{S3}$$

where μ is viscosity, and $r_{0,i}$ and $r_{\mathrm{c},i}$ are length and diameter of an element, respectively. To update the positions of all cylindrical elements at each time step, we employed the Euler integration scheme:

$$\mathbf{r}_i(t+\Delta t) = \mathbf{r}_i(t) + \frac{\mathrm{d}\mathbf{r}_i}{\mathrm{d}t}\Delta t = \mathbf{r}_i(t) + \frac{1}{\zeta_i}\left(\mathbf{F}_i + \mathbf{F}_i^{\mathrm{T}}\right)\Delta t \tag{S4}$$

Deterministic forces

Deterministic forces include extensional and bending forces that maintain equilibrium lengths and equilibrium angles as well as repulsive forces accounting for volume-exclusion effects between membrane elements and cylindrical elements that represent fibers and cross-linkers. Extensional and bending forces for fibers and cross-linkers originate from harmonic potentials:

$$U_{\mathrm{s}} = \frac{1}{2}\kappa_{\mathrm{s}}(r - r_0)^2 \tag{S5}$$

$$U_{\mathrm{b}} = \frac{1}{2}\kappa_{\mathrm{b}}(\theta - \theta_0)^2 \tag{S6}$$

where κ_{s} and κ_{b} are extensional and bending stiffnesses, r and r_0 are the instantaneous and equilibrium lengths of cylindrical elements, and θ and θ_0 are instantaneous and equilibrium angles formed by adjacent elements.

The equilibrium length of fiber elements ($r_{0,\mathrm{f}}$= 1 μm) and an equilibrium angle formed by two adjacent fiber elements ($\theta_{0,\mathrm{f}}$ = 0 rad) are maintained by extensional ($\kappa_{\mathrm{s,f}}$) and bending stiffnesses ($\kappa_{\mathrm{b,f}}$) of fibers, respectively. The value of $\kappa_{\mathrm{b,f}}$ used in the model corresponds to the persistence length of ~100 μm. The equilibrium length of a cross-linker arm ($r_{0,\mathrm{xl}}$ = 200 nm) is maintained by extensional stiffness ($\kappa_{\mathrm{s,xl}}$), and an equilibrium angle between two arms of each cross-linker ($\theta_{0,\mathrm{xl},1}$ = 0 rad) and an equilibrium angle between a cross-linker arm and the axis of a fiber where the arm is bound ($\theta_{0,\mathrm{xl},2}$ = π/2 rad) are maintained by two bending stiffnesses ($\kappa_{\mathrm{b,xl},1}$ and $\kappa_{\mathrm{b,xl},2}$). Forces exerted on a fiber element by bound cross-linkers are distributed onto two nodes located at the ends of the fiber element.

An equilibrium angle formed by adjacent membrane elements ($\theta_{0,\mathrm{m}}$ = 0 rad) is maintained by bending stiffness ($\kappa_{\mathrm{b,m}}$), and the equilibrium length of membrane elements ($r_{0,\mathrm{m}}$ = 400 nm) is

maintained by extensional stiffness ($\kappa_{s,m}$). In addition, an equilibrium angle defined by adjacent cortex elements ($\theta_{0,c}$ = 0 rad) is regulated by bending stiffness ($\kappa_{b,c}$), and the equilibrium length of cortex elements ($r_{0,c}$ = 0 nm) is maintained by extensional stiffness ($\kappa_{s,c}$). Due to the zero equilibrium length, the cortex always behaves as a contractile element.

Membrane and cortex elements located adjacently attract each other to maintain proximity between them. Then, the attractive forces are determined by a harmonic potential (U_{mc}):

$$U_{mc} = \begin{cases} \frac{1}{2}\kappa_{mc}\left(r_{mc} - r_{0,mc}\right)^2 & \text{if} \quad r_{mc} < r_{mc,0} \\ 0 & \text{if} \quad r_{mc} \geq r_{mc,0} \end{cases} \tag{S7}$$

where κ_{mc} is the strength of the attractive force, and r_{mc} and $r_{0,mc}$ are instantaneous and equilibrium distances between membrane and cortex elements.

Repulsive forces between membrane elements and the elements representing matrix fibers and cross-linkers prevent the matrix elements from entering the inner space of the membrane. A minimum distance between a membrane element and a cylindrical element accounting for fibers or cross-linkers, r_r, is computed, and the repulsive force originates from the following harmonic potential (U_r):

$$U_r = \begin{cases} \frac{1}{2}\kappa_r\left(r_r - r_{0,r}\right)^2 & \text{if} \quad r_r < r_{0,r} \\ 0 & \text{if} \quad r_r \geq r_{0,r} \end{cases} \tag{S8}$$

where κ_r is strength of repulsive force, and $r_{0,r}$ is a critical distance.

Fiber formation

Formation of matrix fibers is initiated by a nucleation event with the appearance of one cylindrical element within the computational domain in a random direction perpendicular to the z direction. Polymerization of fibers is simulated by the addition of one cylindrical element to either end of existing fibers. The initial length of cylindrical elements used for the nucleation and polymerization events is 1 μm. Depolymerization of the fibers is not considered. Therefore, if all fiber elements are used for the nucleation and polymerization, there is no more change in the length of each fiber. We adjusted the rates of nucleation and polymerization events depending on fiber element concentration in order to set average fiber length at ~10 μm; without such adjustment, fibers tend to become shorter.

Details of cross-linkers dynamics

Cross-linkers exist in one of the three states: monomeric, inactive, and active states. Initially, all cross-linkers exist in the monomeric state. Monomeric cross-linkers are considered implicitly via their local concentration without explicit positions. Using the binding rate constant ($k_{bd,0}$) and the local concentration, the rate of binding between implicit cross-linkers and fiber elements is calculated. After they bind to binding sites located every 100 nm on fiber elements, they become explicit elements with their own center positions and one arm. The arm formed between the center point of a cross-linker and the binding site is 200 nm in length and perpendicular to the fiber element where the arm is bound. These cross-linkers in the inactive state can bind to a binding site on other fiber elements at the rate of $k_{bd,0}$ if a distance between the center point of the cross-linker and the binding site is between 180 nm and 220 nm. Then, the cross-linkers form the second arm between their center point and the binding site to create a cross-linking

point between pairs of fibers. The unbinding event on two binding points of the active cross-linkers is considered at each time step. Unlike the binding rate, an unbinding rate is dependent on forces applied to cross-linkers as explained in the main text. If the unbinding event occurs, cross-linkers become inactive ones. They can return to the active state if they bind to binding sites on neighboring fiber elements or become monomeric cross-linkers if another unbinding event occurs on a remaining arm subsequently. Despite the transitions of cross-linkers between the three states, the number (or density) of cross-linkers in the active state largely remains at constant level for the entire duration of simulations, meaning their dynamic steady state.

Experimental methods

i) Cell culture and encapsulation in 3D collagen gels: 3T3 mouse fibroblast cells (ATCC) were stably transfected with a PiggyBac vector containing RFP-Lifeact to make a clonal 3T3:RFP-Lifeact cell line as described previously[3]. 3T3:RFP-Lifeact cells were cultured in DMEM (Hyclone) with 10% fetal bovine serum (Hyclone) and 1% Pen/Strep (Thermo Fisher Scientific). For 3D cell encapsulation, collagen type I (Corning) was prepared on ice by first neutralizing collagen stock (3.28 mg/mL or 9.5 mg/mL stock concentration) with 10× Dulbecco's modified Eagle's medium (DMEM) to achieve a pH of 7.4. Then appropriate volume of 1× DMEM with cells was added to bring the final collagen concentration to either 1, 2, 3 or 5 mg/mL, with a final cell concentration of 0.2 million cells per mL. 300μL of final collagen solution was deposited per micro-well of glass bottom 6-well plates (cat. # P06-14-1.5-N, Cellvis) which were coated with 0.01% poly-L-lysine solution (Sigma Aldrich) to improve attachment of collagen to the plate. The

6-well plate was then incubated at 37°C and 5% CO_2 for 25 min to allow gelation, following which growth media was added to the 6-well plate.

ii) Covalent cross-linking of collagen gels: To covalently cross-link collagen gels, tissue transglutaminase from guinea pig liver (cat. # T5398, Sigma Aldrich; 2.2 UN/mg) was used as a cross-linking agent. Collagen type I (Corning) was diluted to 1 mg/mL using transglutaminase. In brief, transglutaminase powder was dissolved in 50 mM Tris Buffer (pH 7.4) to make a stock solution of 1 mg/mL. Prior to mixing with collagen stock solution (3.28 mg/mL stock concentration), 1 mg/mL transglutaminase solution was treated for 10 min at room temperature with a small quantity of 500 mM dithiothreitol (DTT) solution such that the final concentration of DTT was 2 mM. Then, 50 mM calcium chloride ($CaCl_2$) was added to achieve a final concentration of 5 mM $CaCl_2$ to activate the transglutaminase. An appropriate volume of this mix was added to collagen stock solution on ice and mixed thoroughly while avoiding air bubbles to achieve the desired concentration of transglutaminase. Appropriate volume of DMEM with cells was added to bring the final concentration of collagen to 1 mg/mL and that of transglutaminase to 500 µg/mL with a final cell concentration of 0.2 million cells per mL.

iii) Inhibition studies: Inhibitors were used to test the role of actomyosin contractility on collagen remodeling by 3T3 fibroblasts. Inhibitor concentrations used are as follows: 25µM ML-7 to inhibit myosin light chain kinase activity (Tocris) and 10 µM Blebbistatin (Abcam). ML-7 and Blebbistatin were each added to respective gels after encapsulation and imaging was performed 24-hour post encapsulation.

iv) Imaging cells and collagen fiber architecture: Images of collagen fibers were taken using confocal reflectance microscopy (Leica SP8) with a 25×/0.95 NA water immersion objective at a wavelength of 639 nm. Fluorescence imaging of fluorescently labeled F-actin was done using the same objective.

v) Image analysis and statistical analysis: To quantify collagen remodeling by 3T3 fibroblasts, reflectance images of collagen networks were analyzed using ImageJ (NIH). Briefly, for a given cell, pixel intensity was averaged and measured along three independent 40μm-thick lines drawn from the cell edge, away from the cell. Next, average pixel intensity for the collagen network at distance of >200μm away from the same cell was quantified to estimate the average pixel intensity for non-remodeled collagen matrix. This number was then used to normalize and plot intensity of collagen fibers as a function of distance away from cell edge.

Statistical analyses were performed using GraphPad Prism software. Appropriate tests were applied to compare data and corresponding post hoc comparisons were performed to compare experimental groups. Statistical tests performed and corresponding p and n values are specified in the legends of respective figures. P values less than 0.05 were considered statistically significant.

Supplementary references

1. P. T. Underhill and P. S. Doyle, *J Non-Newton Fluid*, 2004, **122**, 3-31.
2. R. Clift, J. R. Grace and M. E. Weber, *Bubbles, drops, and particles*, Courier Corporation, 2005.
3. S. Nam, J. Lee, D. G. Brownfield and O. Chaudhuri, *Biophys J*, 2016, **111**, 2296-2308.

SUPPLEMENTARY TABLE

List of parameters employed in the computational model. The superscript "*" indicates the reference values of parameters.

Symbol	Definition	Value
$r_{0,f}$	Equilibrium length of fibers	1.0×10^{-6} [m]
$r_{c,f}$	Diameter of fibers	6.0×10^{-8} [m]
$\theta_{0,f}$	Bending angle formed by adjacent fibers	0 [rad]
$\kappa_{s,f}$	Extensional stiffness of fibers	2.0×10^{-3} [N/m]
$\kappa_{b,f}$	Bending stiffness of fibers	4.14×10^{-19} [N·m]
$r_{0,xl}$	Equilibrium length of a cross-linker arm	2.0×10^{-7} [m]
$r_{c,xl}$	Diameter of a cross-linker arm	1.0×10^{-8} [m]
$\theta_{0,xl,1}$	Bending angle formed by two cross-linker arms	0 [rad]
$\theta_{0,xl,2}$	Bending angle formed by a cross-linker arm and the axis of a fiber where the arm is bound	$\pi/2$ [rad]
$\kappa_{s,xl}$	Extensional stiffness of cross-linkers	2.0×10^{-3} [N/m]
$\kappa_{b,xl,1}$	Bending stiffness 1 of cross-linkers	1.04×10^{-19} [N·m]
$\kappa_{b,xl,2}$	Bending stiffness 2 of cross-linkers	1.04×10^{-19} [N·m]
$r_{0,m}$	Equilibrium length of membrane elements	4.0×10^{-7} [m]
$\theta_{0,m}$	Bending angle formed by adjacent membrane elements	0 [rad]
$\kappa_{s,m}$	Extensional stiffness of membrane	1.0×10^{-4} [N/m]
$\kappa_{b,m}$	Bending stiffness of membrane	1.0×10^{-18} [N·m]
$r_{i,c}$	Initial length of cortex elements	4.0×10^{-7} [m]
$r_{0,c}$	Equilibrium length of cortex elements	0 [m]
$\theta_{0,c}$	Bending angle formed by adjacent cortex elements	0 [rad]
$\kappa_{s,c}$	Extensional stiffness of cortex (= cortical contraction strength)	1×10^{-3} [N/m] ($=\kappa_{s,c}^{*}$)
$\kappa_{b,c}$	Bending stiffness of cortex	2×10^{-18} [N·m]
$r_{0,mc}$	Equilibrium distance between membrane and cortex	2.5×10^{-7} [m]
$\kappa_{0,mc}$	Strength of attractive force between membrane and cortex	1.6×10^{-3} [N/m]
$r_{0,fc}$	Equilibrium length of links between fibers and cortex	4×10^{-7} [m]
$\kappa_{0,fc}$	Extensional stiffness of links between fibers and cortex	1×10^{-4} [N/m]
κ_{r}	Strength of repulsive force	4×10^{-4} [N/m]
$<L_f>$	Average length of fibers	~10 [μm]
N_m	Number of membrane elements	156
N_c	Number of cortex elements	156
C_f	Fiber density	~0.25 [fiber/μm^3] ($=C_f^{*}$)
R_{xl}	Cross-linking density	~15 [cross-linker/fiber] ($=R_{xl}^{*}$)
$k_{bd,0}$	A binding rate constant of cross-linkers	100 [s^{-1}]
$k_{ub,0}$	Zero-force unbinding rate constant of cross-linkers	1×10^{-6} [s^{-1}] ($=k_{0,u}^{*}$)
x_{ub}	Force sensitivity of cross-linker unbinding	4.0×10^{-10} [m] ($=x_{ub}^{*}$)
Δt	Time step	3.97×10^{-4} [s]
μ	Viscosity of medium	8.6 [Pa·s]
k_BT	Thermal energy	4.142×10^{-21} [J]

SUPPLEMENTARY FIGURES

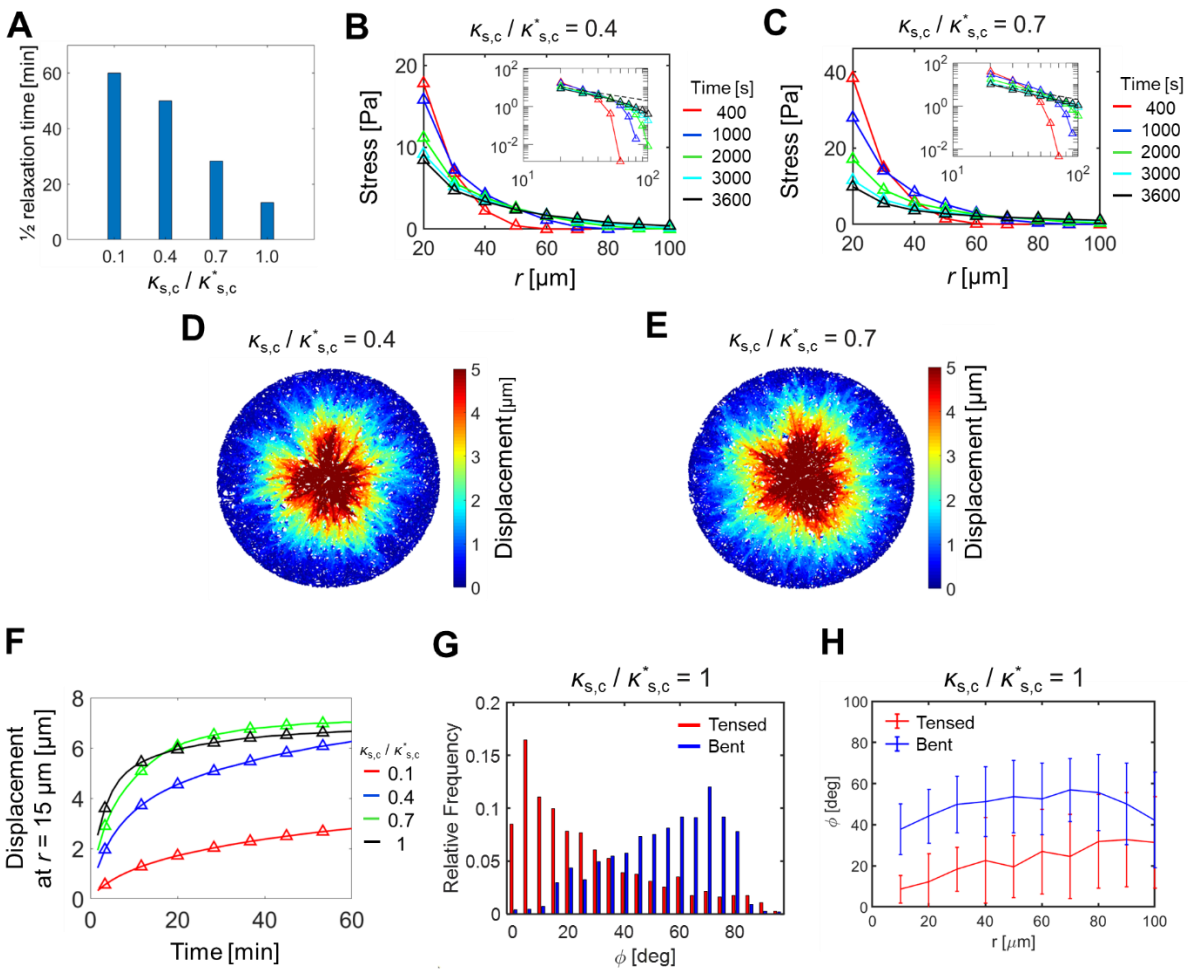

Figure S1. Effects of the strength of cortical contraction, $\kappa_{s,c}$, on stress profiles and matrix remodeling. (A) Time required for peak stress to relax to half level. Note that stress with the smallest $\kappa_{s,c}$ did not reach the half level before 1 h, so 1 h was plotted for the relaxation time. (B, C) Stress exerted on a matrix in radial directions at different time points (legends), depending on a distance from the cell center, r, with two different values of $\kappa_{s,c}$. Insets: the stress in the log-log scale. Dashed lines indicate r^{-1}. (D, E) Fiber displacements at the end of simulations with two values of $\kappa_{s,c}$. (F) Time evolution of average fiber displacement measured at $r = 15$ μm with various values of $\kappa_{s,c}$. (G) The distribution of the orientations of buckled (blue) and tensed (red) fibers measured with respect to radial directions at the end of simulations with the reference value of $\kappa_{s,c}$. (H) The mean and standard deviation of the orientations of buckled (blue) and tensed (red) fibers as a function of a distance from the cell center, r. Note that $\kappa^*_{s,c}$ is the reference value of $\kappa_{s,c}$.

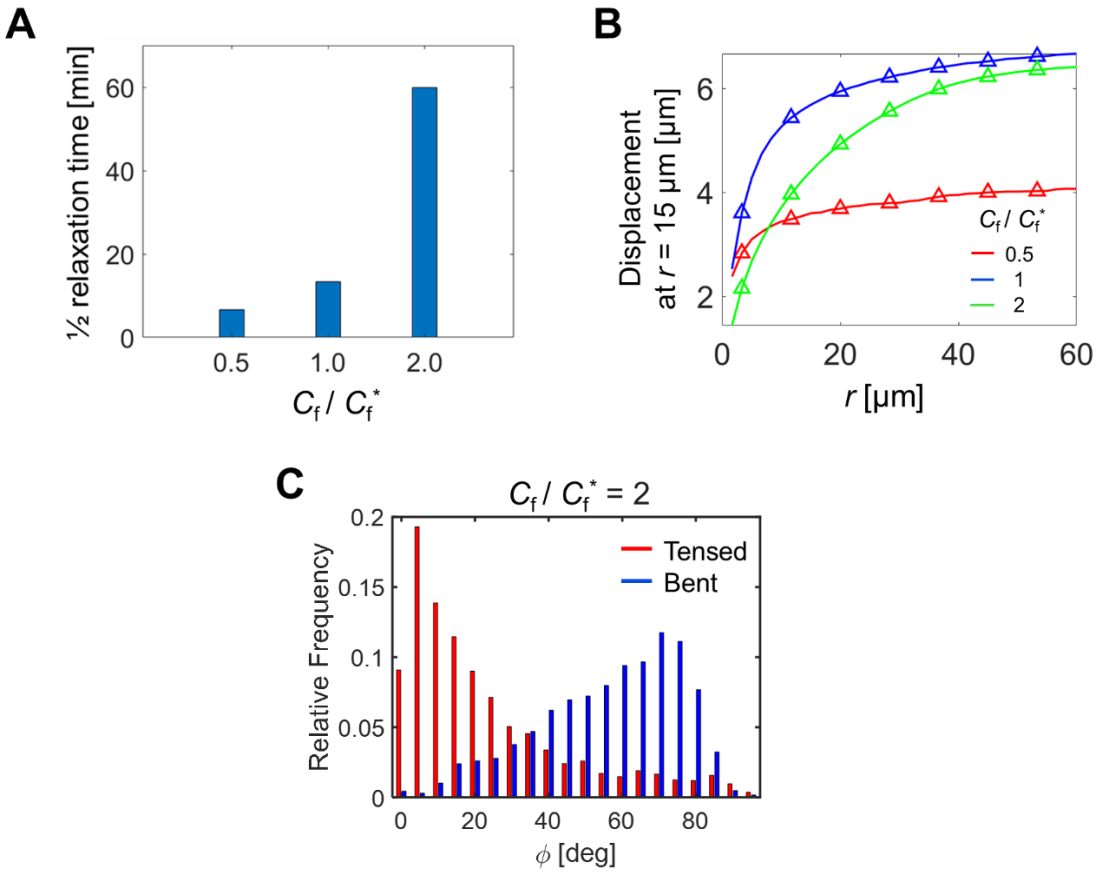

Figure S2. The influence of fiber density, C_f, on the displacement and orientations of fibers. (A) Time required for peak stress to relax to half level. Note that stress with the largest C_f did not reach the half level before 1 h, so 1 h was plotted for the relaxation time. (B) Time evolution of the average displacement of fibers measured at r = 15 μm with three different values of C_f. (C) The distribution of the orientations of buckled (blue) and tensed (red) fibers measured with respect to radial directions at the end of simulations with larger C_f. Note that C^*_f is the reference value of C_f.

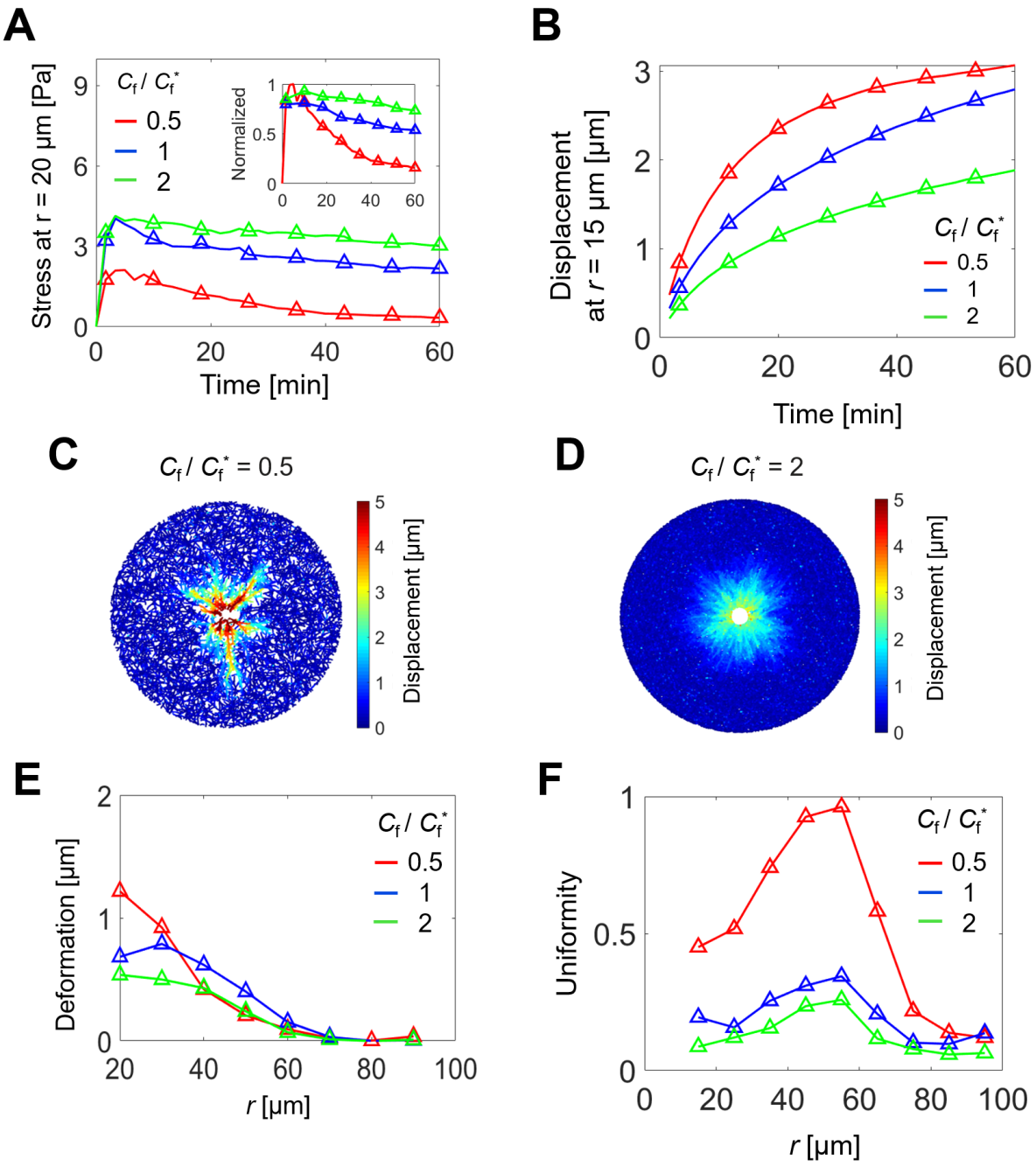

Figure S3. The effects of fiber density, C_f, on matrix remodeling and stress profiles with 10-fold lower contraction strength. (A) Time evolution of stress at r = 20 μm with different C_f as a function of a distance from the cell center, r. Inset: stress normalized by peak level. (B) Time evolution of the average displacement of fibers calculated at r = 15 μm with three values of C_f. (C, D) The distribution of fiber displacements visualized via color scaling with two values of C_f. (E) Net local matrix deformation and (F) the anisotropy of the matrix deformation as a function of r and C_f. Note that C^*_f is the reference value of C_f.

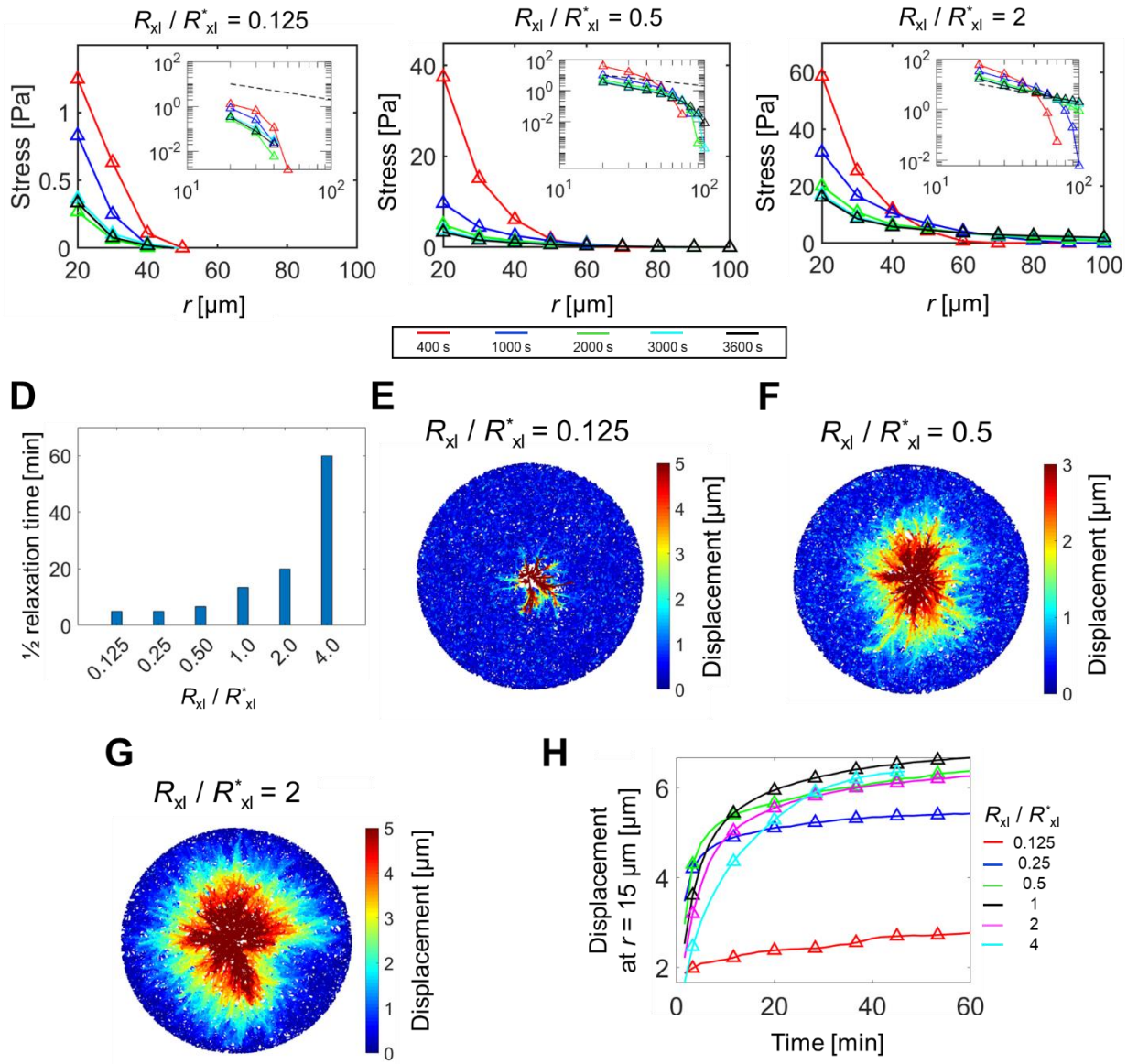

Figure S4. The influences of cross-linking density, R_{xl}, on matrix deformation and the generation, propagation and relaxation of stress. (A-C) Stress exerted on the matrix in radial directions at different time points (legend), as a function of a distance from the cell center, *r*, with three different values of R_{xl}. Inset: stress in the log-log scale. Dashed lines represent r^{-1}. Insets: stress in the log-log scale. Dashed lines indicate r^{-1}. (D) Time required for peak stress to relax to half level. (E-G) Visualization of fiber displacements at the end of simulations with three values of R_{xl}. (H) Time evolution of the average fiber displacement at r = 15 μm with various values of R_{xl}. Note that R^*_{xl} is the reference value of R_{xl}.

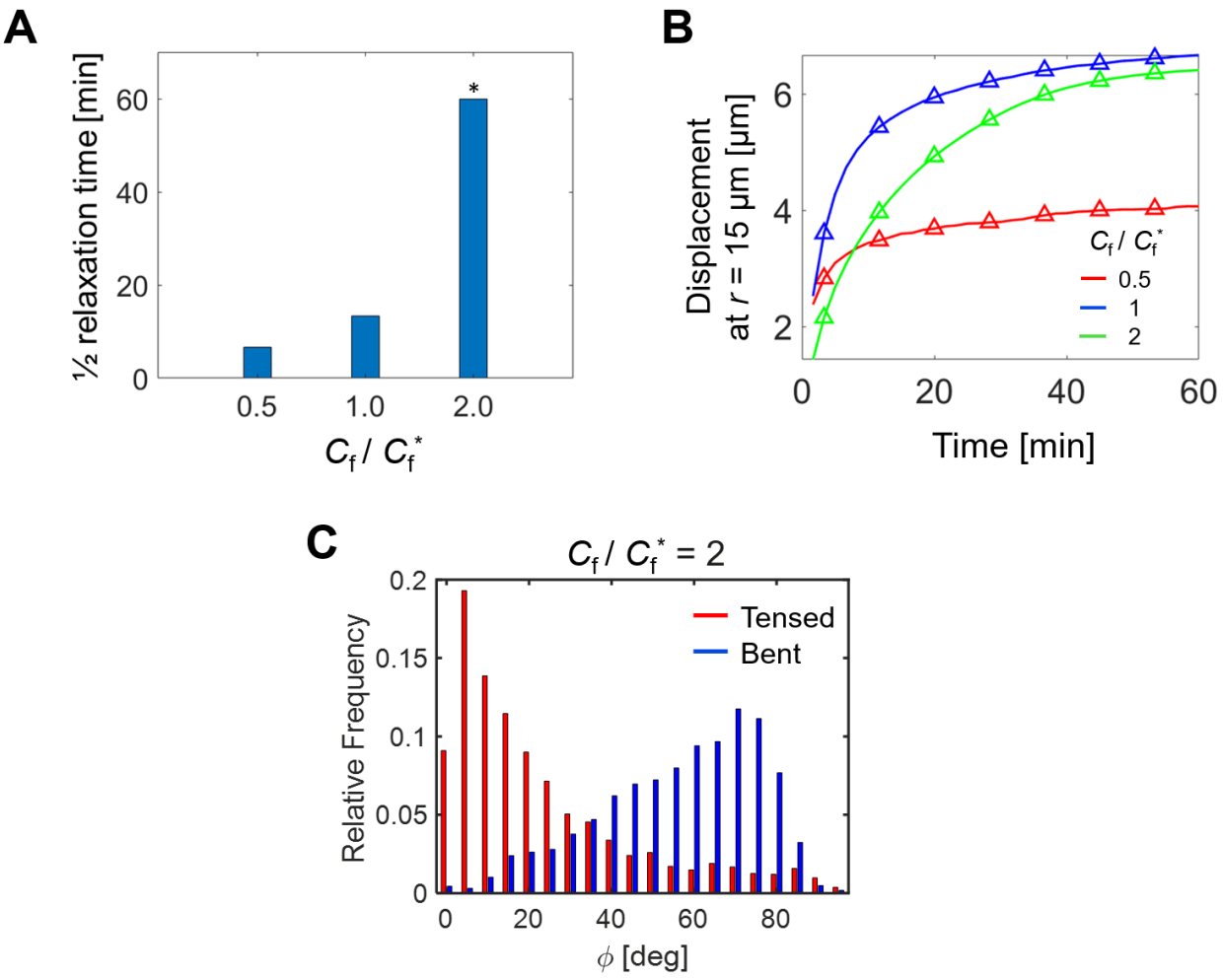

Figure S5. The effects of the zero-force unbinding rate constant in Bell's equation, $k_{ub,0}$, on fiber displacement and stress profiles. (A) Time required for peak stress to relax to half level. (B) Stress acting on the matrix in radial directions at different time points (legend), as a function of a distance from the cell center, r, with $k_{ub,0} / k_{ub,0}^* = 10$. Inset: the same stress curves in the log-log scale. A dashed line indicates r^{-1}. (C) Fiber displacements measured at the end of simulations.

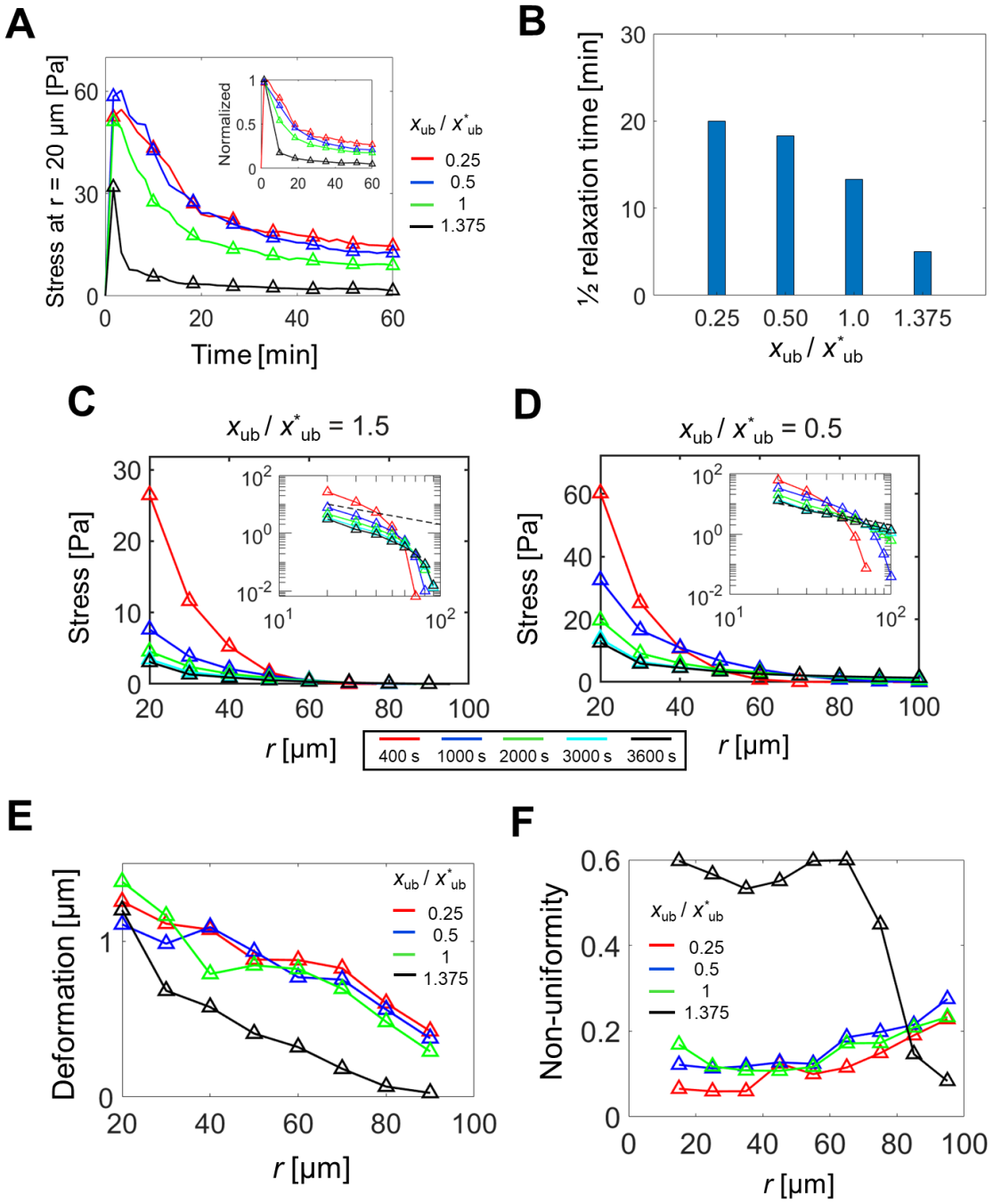

Figure S6. The influences of the force sensitivity in Bell's equation, x_{ub}, on matrix remodeling and stress. (A) Relaxation of the stress calculated at r = 20 μm with four values of x_{ub}. (B) Time required for peak stress to relax to half level. (C, D) Stress exerted on the matrix in radial directions at five different time points (legend), depending on a distance from the cell center, r. Insets: stress shown in the log-log scale. Dashed lines represent r^{-1}. (E) Net matrix deformation and (F) the anisotropy of the matrix deformation, as a function of r and x_{ub}. Note that x^*_{ub} is the reference value of x_{ub}.

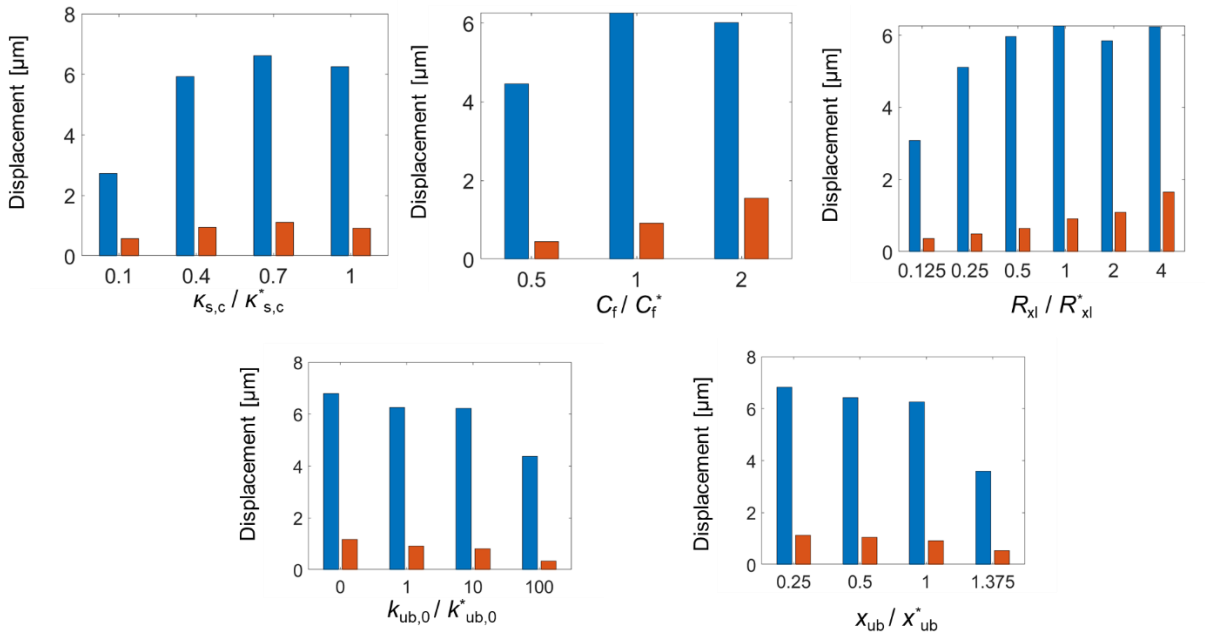

Figure S7. Evaluation of elastic, reversible deformation and irreversible, plastic deformation. In all parts, blue bars show the average inward displacement of fibers, initially located at 0-20 μm from the cell center, induced by cell contraction. Red bars show the radially outward retraction of fibers, located at 0-20 μm from the cell center at 1 h, after disconnection between the cell and the matrix. If matrix deformation is very elastic, two bars would look similar to each other. In cases with different (A) cell contraction strength, (B) fiber density, (C) cross-linking density, (D) zero-force unbinding rate constant, and (E) force sensitivity of cross-linker unbinding, fiber displacement induced by retraction is much smaller than that induced by contraction, meaning that matrix remodeling was mostly irreversible and plastic. The degree of reversible matrix deformation was larger with higher fiber concentration, higher cross-linking density, and slower cross-linker unbinding because a matrix tends to be more elastic under such conditions.